

Redox strategy for reversible attachment of biomolecules using bifunctional linkers

Galina V. Dubacheva*, Mathieu Galibert, Liliane Guerente, Pascal Dumy, Didier Boturyn and Pierre Labbé*

Supporting information

Experimental section

1. Synthesis of tetravalent Fc-biotin linker

All Fmoc amino acid derivatives and resins were purchased from Advanced ChemTech Europe (Brussels, Belgium), Bachem Biochimie SARL (Voisins-Les-Bretonneux, France) and France Biochem S.A. (Meudon, France). PyBOP was purchased from France Biochem and other reagents were obtained from either Aldrich (Saint Quentin Fallavier, France) or Acros (Noisy-Le-Grand, France). RP-HPLC was performed on Waters system equipped with a Waters 600 controller and a Waters 2487 Dual Absorbance Detector. The purity of peptide derivatives was analyzed on an analytical column (Macherey-Nagel Nucleosil 120 Å 3 µm C18 particles, 30x4.6 mm) using the following solvent system: solvent A, water containing 0.09% TFA; solvent B, acetonitrile containing 0.09% TFA and 9.91% H₂O; flow rate of 1.3 mL/min was employed with a linear gradient (5 to 100% B in 15 min). UV absorbance was monitored at 214 nm and 250 nm simultaneously. Preparative column (Delta-Pak™ 100 Å 15 µm C18 particles, 200x2.5 mm) was used to purify the crude peptides (when necessary) by using an identical solvent system at a flow rate of 22 mL/min. ESI mass spectra were recorded on an Esquire 3000 (Bruker) spectrometer. The analysis was performed in the positive mode for peptide derivatives using 50% aqueous acetonitrile as eluent.

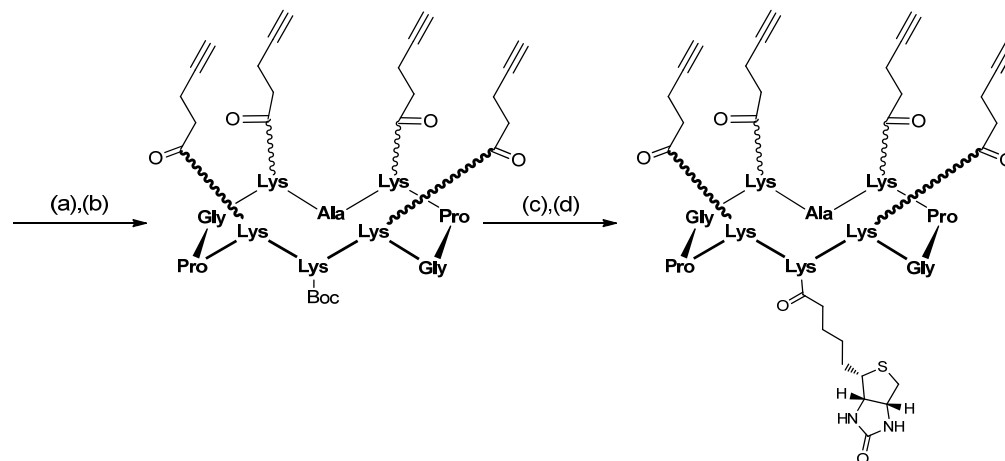
1.1. General Procedure for Solid-Phase Peptide Synthesis

Assembly of all protected peptides was carried out using the Fmoc/*t*-Bu strategy manually in a glass reaction vessel fitted with a sintered glass frit or automatically on a peptide synthesizer using 2-chlorotriylchloride[®]. Coupling reactions were performed manually by using 2 equiv. of *N*-Fmoc-protected amino acid (relative to the resin loading) activated in situ with 2 equiv. of PyBOP and 3-5 equiv. of diisopropylethylamine (DIPEA) in DMF (10 mL/g resin) for 30 min except for the first coupling on 2-chlorotriylchloride[®]. Coupling reactions carried out on the synthesizer were performed twice. The coupling efficiency in manual synthesis was assessed by Kaiser and/or TNBS tests. *N*-Fmoc protecting groups were removed by treatment with a piperidine/DMF solution (1:4) for 10 min (10 mL/g resin). The process was repeated three times and the completeness of deprotection verified by UV absorption of the piperidine washings at 299 nm. Synthetic linear peptides were recovered directly upon acid cleavage. Before cleavage, the resin was washed thoroughly with methylene chloride. The linear peptides were then released from the resin by treatments with a solution of acetic acid/trifluoroethanol/methylene chloride (1:1:8, 10 mL/mg resin, 2x30 min). Hexane (5-10 volumes) was added to the collected filtrates, and the crude peptides were isolated after evaporation as white solids. The residue was dissolved in the minimum of methylene chloride and diethyl ether was added to precipitate peptides. Then they were triturated and washed three times with diethyl ether to obtain crude materials that were used in the next step without further purification.

1.2. General Procedure for Cyclization Reactions

All linear peptides (0.5 mM) were dissolved in DMF and the pH values were adjusted to 8-9 by addition of DIPEA. PyBOP (1 equiv.) was added and the solution stirred at room temperature for 1 h. Solvent was removed under reduced pressure and the residue dissolved in the minimum of methylene chloride. Et₂O was added to precipitate peptides. Then they were triturated and washed three times with diethyl ether to obtain crude materials that were used in the next step without further purification.

1.3. Synthesis of cyclodecapeptide scaffold



Reagents and conditions: (a) SPPS; (b) PyBOP, DIPEA, DMF; (c) TFA/TIS/H₂O (96/2/2); (d) Biotin, PyBOP, DIPEA, DMF.

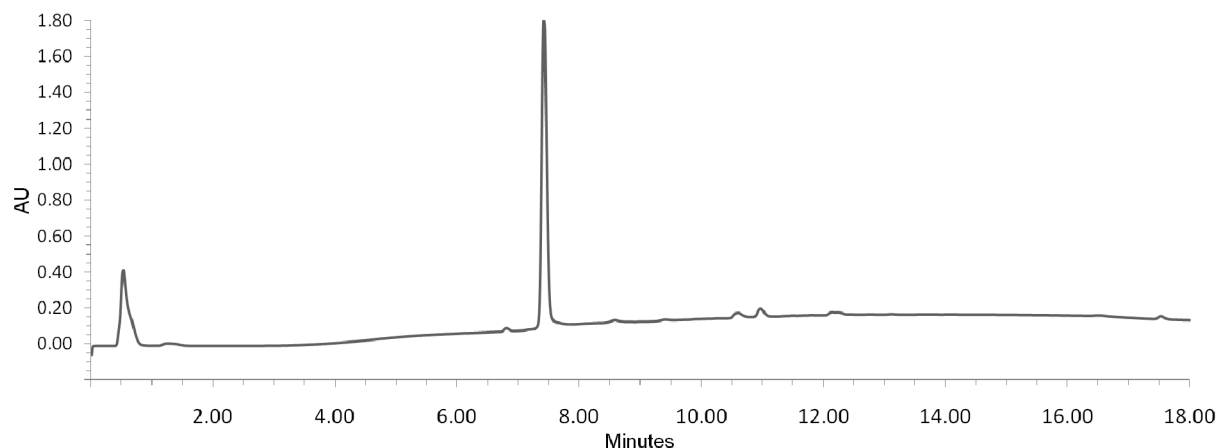
The linear decapeptide was assembled on 2-chlorotriylchloride[®] resin (150 mg, loading of 1.1 mmol/g) using the general procedure and modified amino acid Fmoc-Lys[N-4-Pentynoic acid]-OH.¹ The anchoring of the first amino acid (Fmoc-Gly-OH) was performed following the standard procedure yielding a convenient resin loading of 0.7 mmol/g. The peptide was released from the resin using cleavage solution of TFA/DCM (1:99). Linear protected peptide was obtained as a white solid powder after precipitation, triturating and washing with Et₂O.

The cyclization reaction was carried out as described in general procedure using the crude linear peptide. Precipitation from Et₂O afforded cyclic peptide as a white solid powder (150 mg, 100 μmol, quantitative). Mass spectrum (ES-MS, positive mode) calc for C₇₂H₁₀₉N₁₅O₁₆ 1440.8, found m/z: 1440.7.

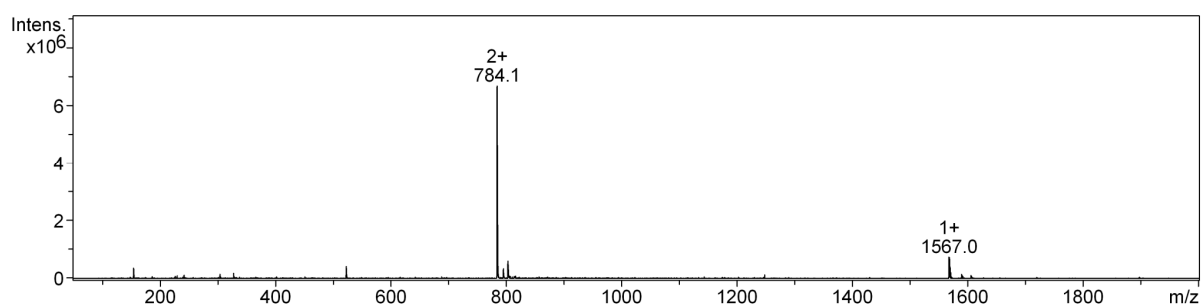
The cyclopeptide (150 mg, 100 μmol) was dissolved in 15 mL of TFA/TIS/H₂O (96/2/2) solution. The reaction mixture was stirred for 1 h at room temperature. The product was concentrated under reduced pressure and precipitate from Et₂O afforded the raw peptide as a white solid powder. Then, 1.2 equiv. of Biotin (29.3 mg, 120 μmol) and 1.2 equiv. of PyBOP (62.4 mg, 120 μmol) were added to a solution containing the crude peptide in 10 mL of DMF. The pH was adjusted at 8.0 using DIPEA and the reaction was stirred for 30 min at room temperature. The product was concentrated under reduced pressure and precipitate from Et₂O afforded the raw peptide as a white solid powder. This crude material was purified by RP-HPLC affording the pure **cyclodecapeptide scaffold** as a white powder (71 mg, 45 μmol, 45%).

Mass spectrum (ES-MS, positive mode) calc for C₇₇H₁₁₅N₁₇O₁₆S 1566.9, found m/z: 1567.1.

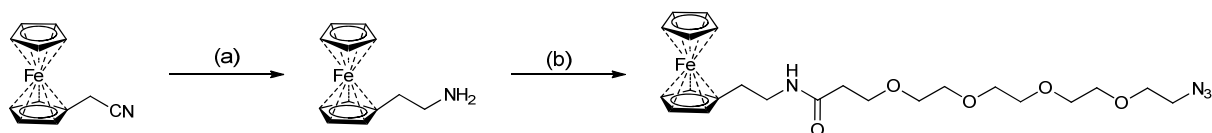
RP-HPLC profile of cyclodecapeptide scaffold



ESI-MS analysis of cyclodecapeptide scaffold



1.4. Synthesis of Fc-PEG(4)-N₃

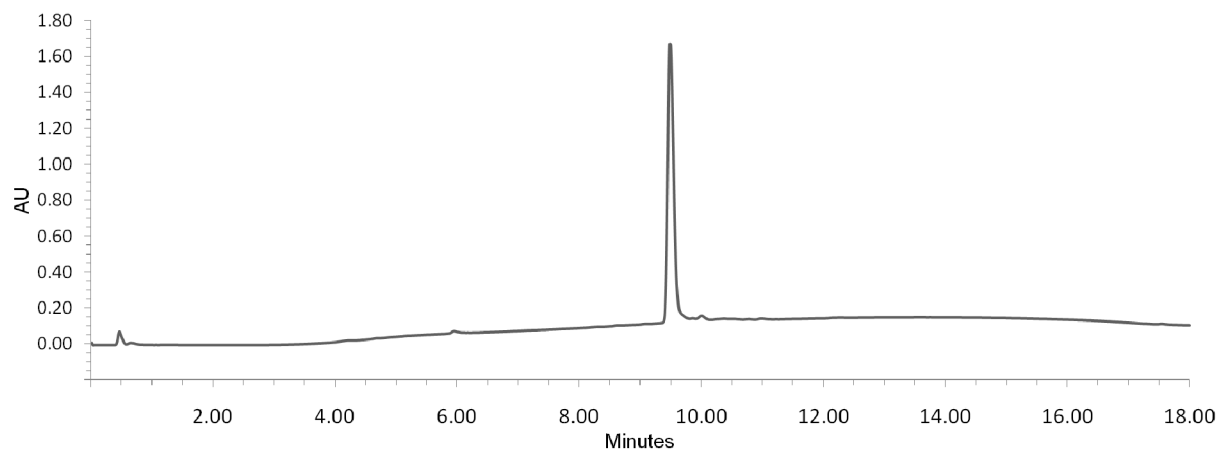


Reagents and conditions: (a) $\text{LiAlH}_4, \text{AlCl}_3, \text{THF}$ (b) $\text{N}_3\text{-PEG}(4)\text{-NHS}$, DMF , DIPEA

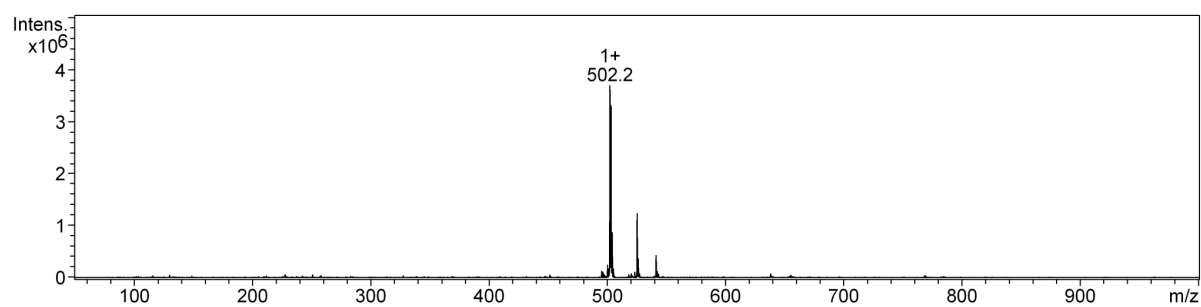
3 equiv. of LiAlH_4 (250mg, 6.6 mmol) and 2 equiv. of AlCl_3 (585mg, 4.5 mmol) were dissolved in 10 mL dry THF while stirring in an ice bath. Ferroceneacetonitrile (0.5 mg, 2.2 mmol) dissolved in 5 mL THF were added and the mixture was refluxed for two hours. After cooling, 20 mL of water was carefully added dropwise to decompose the excess of LiAlH_4 followed by 0.5 mL of NaOH solution (10 M). The aqueous solution was then extracted with Et_2O (4 x 10 mL). The combined organic extracts were dried over MgSO_4 and evaporated to dryness to give a brown oil which was used without purification (250 mg, 1 μmol 49%) $^1\text{H-NMR}$ (400 MHz, DMSO-d_6) δ (ppm) 2.48 (t, 2H), 2.81(t, 2H), 4.00 (s, 4H), 4.05 (s, 5H) Mass spectrum (ES-MS, positive mode) calc for $\text{C}_{12}\text{H}_{15}\text{FeN}$ 229.1, found m/z : 230.0.

To a stirred mixture of 2-Ferroceneethylamine (46 mg, 200 μmol) in DMF (2 mL) was added dropwise over 10 min a solution of $\text{N}_3\text{-PEG}(4)\text{-NHS}$ (50 mg, 130 μmol , purchased from IRIS Biotech GMBH) in DMF (1 mL) at room temperature. The pH of the resulting mixture was regularly adjusted to pH 8-9 by additions of DIPEA. After 2 h of reaction, the product was directly purified by RP-HPLC affording the pure product **Fc-PEG(4)-N₃** as a brown oil (42 mg, 84 μmol , 64%) Mass spectrum (ES-MS, positive mode) calc for $\text{C}_{23}\text{H}_{34}\text{FeN}_4\text{O}_5$ 502.4, found m/z : 502.2.

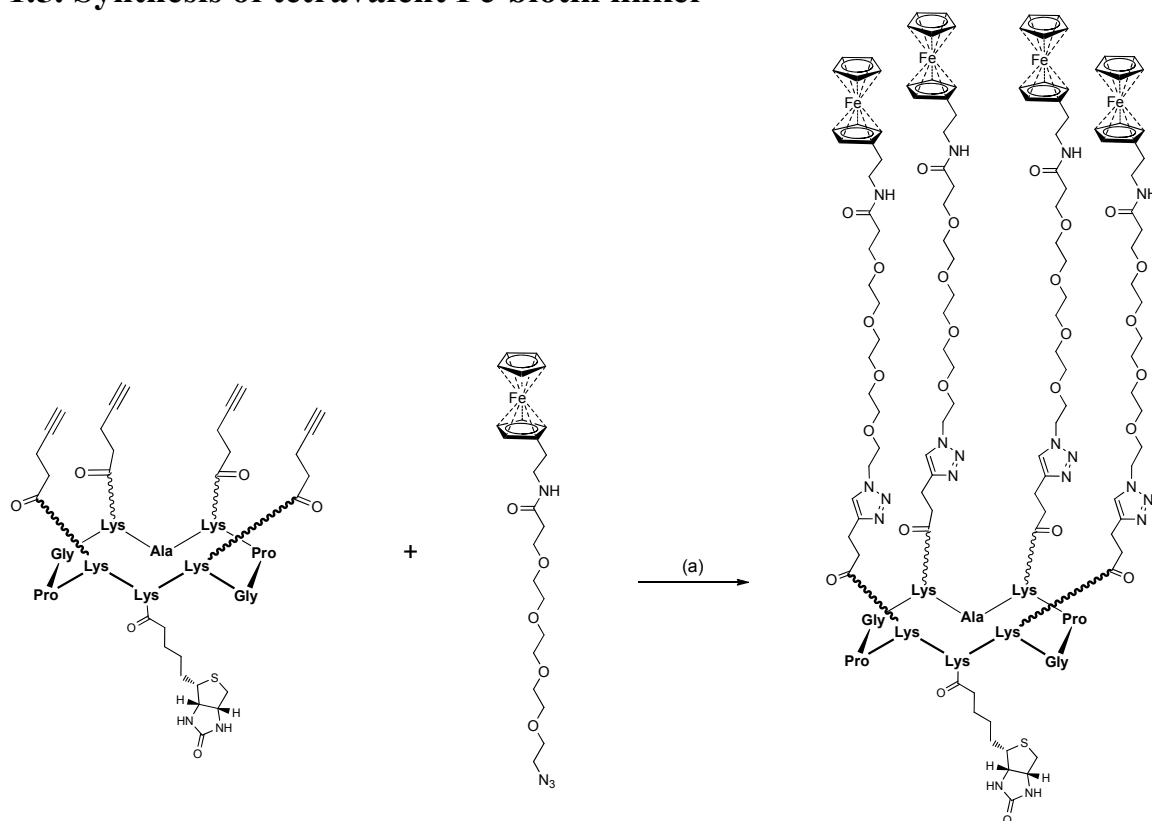
RP-HPLC profile of Fc-PEG(4)-N₃



ESI-MS analysis of compound Fc-PEG(4)-N₃



1.5. Synthesis of tetravalent Fc-biotin linker



Reagents and conditions: (a) CH₃CN/PBS (pH 7), 1 equiv. CuSO₄, 1 equiv. sodium ascorbate, MW, 60°C, 30 min

Cyclodecapeptide scaffold (10 mg, 6.4 μmol), 5 eq. of compound Fc-PEG(4)-N₃ (16 mg, 32 μmol), 1 equiv. of CuSO₄ and 1 equiv. of sodium ascorbate were dissolved in 500 μL *t*BuOH/PBS buffer (6:4, pH 7). The mixture was stirred at 60 °C for 30 min under microwave. The solution was then purified by RP-HPLC to give the desired **tetravalent Fc-biotin linker** as a yellowish powder (14.3 mg, 4 μmol , 63 %) Mass spectrum (ES-MS, positive mode) calc for C₁₆₉H₂₅₁Fe₄N₃₃O₃₆S 3575.5, found 3575.2.

RP-HPLC profile of tetravalent Fc-biotin linker

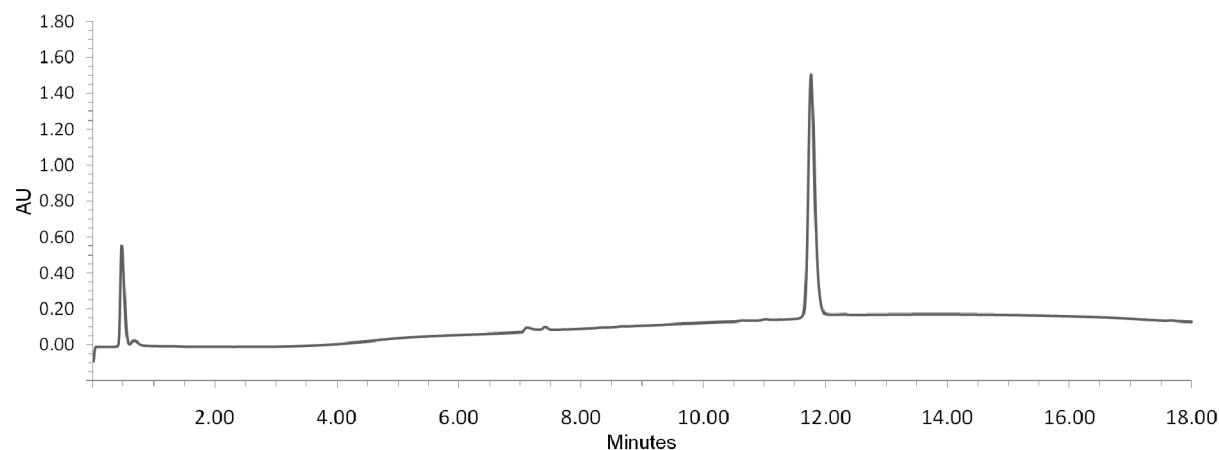
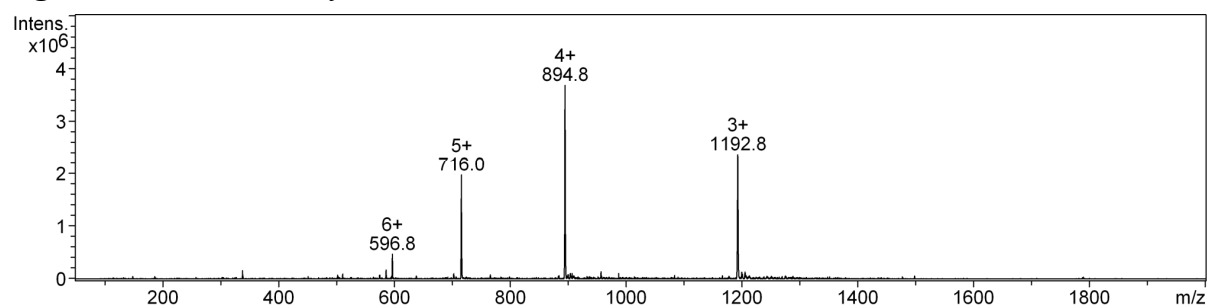


Figure S1 : ESI-MS analysis of tetravalent Fc-biotin linker



2. Formation of β -CD SAMs

The main steps of β -CD SAMs formation, described and characterized in detail elsewhere,² are presented in the following. (Tris[(1-benzyl-1H-1,2,3-triazol-4-yl)methyl]amine (TBTA) was purchased from Aldrich. Sodium ascorbate and CuSO₄·5H₂O were purchased from Alfa Aesar. HS-(CH₂)₁₁-EG₄-OH and HS-(CH₂)₁₁-EG₆-N₃ were purchased from Prochimia. All other chemical products were purchased from Fluka. β -Cyclodextrin (β -CD) was kindly supplied by Roquette Frères (Lestrem, France). β -CD monoalkyne (β -CD-alkyne) was synthesized as described previously.² When mentioned, Milli-Q water (resistivity = 18.2 M Ω ·cm; Millipore system, France) was used as solvent or co-solvent. For simplicity, the terms “thiol-PEG-OH” and “thiol-PEG-N₃” are used to refer to HS-(CH₂)₁₁-EG₄-OH and HS-(CH₂)₁₁-EG₆-N₃, respectively, in the sequel. In QCM-D experiments, gold-coated quartz crystals QSX301 (d_{Au} =100 nm) were used (Q-Sense, Sweden). In ellipsometric experiments, gold-coated SF10 glass slides (d_{Au} =45 nm) were used (Nanofilm, Germany). Cleaning procedure included UV-ozone treatment during 5 min followed by immersion of gold surfaces in ethanol for 20 min with stirring. Preliminarily cleaned gold surfaces were functionalized according to the following procedure. Firstly, mixed self-assembled monolayers (SAMs) were formed at room temperature by dipping overnight gold sensors in the mixture of thiols: 80% HS-(CH₂)₁₁-EG₄-OH and 20% HS-(CH₂)₁₁-EG₆-N₃ (1 mM total thiol concentration in EtOH).

After overnight adsorption of thiols, gold sensors were rinsed with ethanol and dried under nitrogen. Then, click reaction was carried out between azide-terminated SAMs and β -CD-alkyne in order to produce β -CD SAMs. To perform click functionalization, gold electrodes covered with mixed SAMs were immersed in water/*t*-BuOH (1:2) solution containing 1 mM β -CD-alkyne, 1 mM CuSO₄, 1mM TBTA and 7 mM sodium ascorbate for 5 hours. After reaction, monolayers were rinsed with ethanol, water, dichloromethane and then ethanol again to ensure that any physisorbed molecules were washed off.

3. Electrochemistry

Electrochemical experiments were performed with a conventional three-electrode potentiostatic system. The equipment was CHI 440 potentiostat (CH-Instruments, Inc., USA). Electrode potentials were referred to Ag/AgCl/KCl (3M). The counter electrode was platinum and the working electrode was a functionalized gold sensor. Electrochemical detachment was done *in situ* in case of QCM-D (E-QCM-D, see Section 5) and *ex situ* in case of SPR ellipsometry. The *ex situ* electrochemical measurements were performed using home made electrochemical cell. The working, counter and reference electrodes were immersed in 10 mM HEPES buffer containing 0.15 M NaCl (pH 7.0). Electrochemical detachment of the linker and its complex with streptavidin (SA) formed stepwise (linker/SA) was done in the buffer by applying an oxidizing electric field ($E_{ox}=+0.55V$ was used to oxidize attached to the surface ferrocene groups). *In situ* detachment was done by E-QCM-D under flow conditions (50 μ L/min) during 1 \times 5 min (linker) or 2 \times 10 min (linker/SA). *Ex situ* detachment was done in electrochemical cell under stirring during 2 \times 20 min.

4. UV-Visible spectrophotometry

The concentration and the solubility of tetravalent Fc-biotin linker were determined by UV-Visible spectrophotometer Cary 400 (Varian, Inc.). Each measurement was performed using baseline correction option, for which an absorbance spectrum of pure solvent (without the linker) was preliminary measured each time. First 15 mg of the obtained yellowish powder (tetravalent Fc-biotin linker) was dissolved in 1 mL of methanol giving theoretical concentration of 4.2 mM ($M_w = 3576.45$). This solution was measured spectrophotometrically (Fig. S1a). Extinction coefficient measured for ferrocene in methanol is $\epsilon_{440} = 84 \text{ M}^{-1} \text{ cm}^{-1}$.³ Therefore, we used 4-times higher extinction coefficient for tetravalent Fc-biotin linker in methanol ($336 \text{ M}^{-1} \text{ cm}^{-1}$). According to Beer-Lambert law:

$$A = \epsilon l c \tag{1}$$

where A is absorbance, ϵ – extinction coefficient ($\text{M}^{-1} \text{ cm}^{-1}$), l – path length (cm), c – concentration (M), we determined experimentally the concentration of the linker. From the spectrophotometric data (Fig. S1a), $A_{max}=1.417$ yielding $c = 4.2 \text{ mM}$ ($l = 1 \text{ cm}$) that is exactly the linker theoretical concentration. The diluted aqueous solutions of the linker were prepared by injection of a small portion of this solution (several μ L), with concentration of the diluted aqueous solutions being calculated knowing the concentration for the concentrated methanol solution (4.2 mM).

We found that tetravalent Fc-biotin linker is not soluble in aqueous solutions even at very low concentration ($\leq 5 \mu\text{M}$), but became soluble when native β -CD is added (Fig. S1b). Indeed, it was shown for Fc-functionalized dendrimers (containing from 4 to 64 Fc end groups) that free β -CDs are able to form inclusion complexes with all Fc end groups resulting in water-soluble dendrimer- β -CD assemblies.⁴

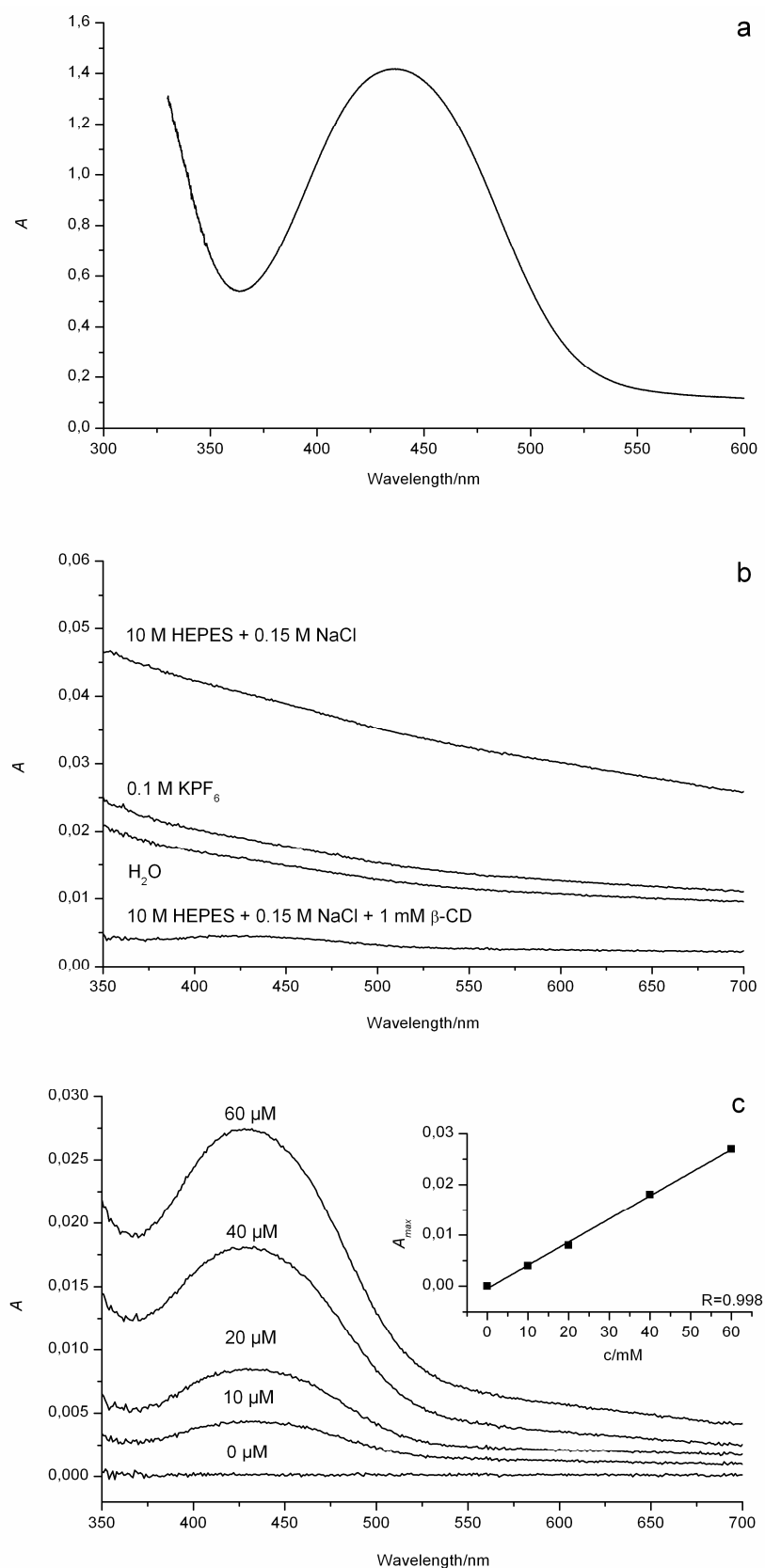


Fig. S1. Absorbance spectra obtained for methanol solution containing 4.2 mM linker **(a)**, different aqueous solutions containing 5 μ M linker **(b)** and 10 mM HEPES buffer with 0.15 M NaCl and with 1 mM β -CD containing different linker concentrations **(c)**. Insert in **(c)**: linear plot obtained from **(c)** data for maximal absorbance as a function of linker concentration, with $\epsilon_{430} = 460 \pm 10 \text{ M}^{-1} \text{ cm}^{-1}$ being calculated from the slope.

All attachment/detachment steps in this work were performed in 10 mM HEPES buffer containing 0.15 M NaCl (pH 7.0). While dissolving tetravalent Fc-biotin linker in this medium, native β -CD (1 mM) was injected into the buffer for the effective linker solubilization. By measuring different linker concentrations in the buffer containing native β -CD (1 mM), we found $\epsilon_{430} = 460 \pm 10 \text{ M}^{-1} \text{ cm}^{-1}$ (Fig. S1c). While keeping aqueous linker solutions in the fridge, we checked their concentration spectrophotometrically using this extinction coefficient.

5. Quartz Crystal Microbalance with Dissipation Monitoring (QCM-D)

QCM-D is an electro-mechanical method based on a piezoelectric effect that allows adsorption processes on a solid surface to be followed in real-time. A piezoelectric quartz crystal is sandwiched between two electrodes and excited into a shear movement by applying an oscillating electric field. The cut off of the electric field results in a damped oscillation curve. Fitting the decay of the damping curve provides information on both, the resonance frequency F_n of the crystal and the degree of damping – the dissipative losses D_n , n being the overtone number. The changes in F_n and D_n are the parameters that are acquired during the measurement. As shown by Sauerbrey in the 1950s,⁵ the adsorbed mass (ΔI) is directly proportional to the frequency change, F_n , of the oscillating sensor crystal, provided the adsorbed film is sufficiently thin, rigid and homogenous:

$$\Delta I = -C \cdot \Delta F_n / n \quad (2)$$

with the mass sensitivity being $C = 17.7 \text{ ng cm}^{-2} \text{ Hz}^{-1}$ for $F_1 = 5 \text{ MHz}$. In solutions, the QCM-D is also sensitive to water that is coupled to the adsorbed molecular film. The mass determined by equation (2) therefore typically exceeds the dry mass of the molecular film.⁶ The change in dissipation, D , is related to frictional (viscous) losses in the adlayer.⁷ D is related to the Q factor, and describes the ratio of stored and dissipated energy in the system (per oscillation cycle):

$$D = 1/Q = E_{\text{dissipated}} / 2\pi E_{\text{stored}} \quad (3)$$

A soft adlayer will not fully couple with the induced shear movement of the crystal, leading to energy dissipation (D increases). For a sufficiently rigid biomolecular film at high coverage, the frequency shift typically corresponds rather well to the molecular (dry) mass together with the mass of the solvent that is contained inside the film.

QCM-D measurements were performed at 24°C using gold-coated ($d_{Au} = 100 \text{ nm}$) quartz crystals QSX301 (Q-Sense, Sweden) with 5 MHz resonant frequency, cleaned and functionalized as described in Section 2. All experiments were performed using QCM-D E4 system equipped with four flow chambers (Q-Sense, Sweden). The overtones $n = 3, 5, 7, 9, 11$ and 13 were recorded in addition to the fundamental resonance frequency to improve stability and sensitivity. Before starting the experiment, resonance frequency and dissipation found for each overtone were set equal to zero. QCM-D measurements were done in flow mode (50 $\mu\text{L}/\text{min}$) using 10 mM HEPES with 0.15 M NaCl (pH 7.0) as a medium. The concentration of streptavidin (SA) in the buffer was 1 mg L^{-1} . Immobilization of the linker and SA was carried out step by step at a flow rate of 50 $\mu\text{L min}^{-1}$. Attachment of both linker and SA was performed during 10 min followed by buffer rinsing (50 $\mu\text{L min}^{-1}$) until stabilization of the acoustical signals. All solutions were thermostated at 24 °C using Thermomixer (Ependorf, France). Combination of electrochemical and QCM-D measurements (E-QCM-D) was performed using electrochemical QCM-D modules (Q-Sense, Sweden), connected with CHI 440 potentiostat (CH-Instruments, Inc., USA) described in Section 3. Electrode potentials were referred to Ag/AgCl/KCl (3M) (Q-Sense, Sweden). The counter electrode was platinum and the working electrode was the modified gold sensor (Q-Sense, Sweden). Working

electrode mounted in electrochemical QCM-D module was covered with the electrolyte solution in which the counter and the reference electrodes were immersed. All QCM-D experiments were repeated at least three times. Data were fitted based on the Sauerbrey equation (2). *Dissipation shifts* (**Manuscript, Fig. 2**) were calculated by subtracting the values recorded just after the attachment and rinsing from the values recorded just before the attachment. The averaged values of several QCM-D experiments were used taking into account dissipation shifts at six overtones.

Fig. S2 illustrates the influence of concentration of tetravalent Fc-biotin linker dissolved in 10 mM HEPES with 0.15 M NaCl (pH 7.0) containing 1 mM β -CD on its attachment at β -CD SAMs. One can see that F_n and D_n shifts obtained just after linker injection during 10 min grow upon increasing linker concentration. In contrast, F_n and D_n shifts obtained after linker injection (10 min) and solvent rinsing (10 min) stop increasing at 5 μ M. This shows that the amount of linker molecules attached to β -CD SAMs through monovalent or labile multivalent host-guest interactions increase in concentration range from 1 to 60 μ M. While the amount of linker molecules strongly attached to β -CD SAMs through stable multivalent host-guest interactions, stable upon solvent rinsing, remains the same starting from 5 μ M. Therefore, we chose 5 μ M as an optimal linker concentration, which was used in all further experiments. Another important result obtained in this experiment is that frequency shifts obtained for the first linker injection/rinsing and the last (8th) one are identical for the same linker concentration (1 μ M). This shows that the linker attachment/detachment procedure can be repeated several times without changing the inclusion properties of β -CD SAMs.

Fig. S3 and S4 show typical QCM-D profiles obtained for the attachment of tetravalent Fc-biotin linker to unmodified pegylated SAMs and SA to β -CD SAMs, respectively. In these experiments, both adsorption and rinsing steps were performed during 10 min according to the procedure used for the specific attachment of the linker to β -CD SAMs and SA to the linker-covered β -CD SAMs. One can see that small shifts in frequency and dissipation during the attachment of the linker to unmodified pegylated SAMs disappear after solvent rinsing (Fig. S3). Fig. S4 illustrates the same F_n and D_n behaviour observed for SA attachment to β -CD SAMs. Therefore, we proved the absence of strong non-specific interactions between linker and β -CD SAMs as well as between SA and linker-modified β -CD SAMs.

We showed (Fig. S2) that the majority of tetravalent Fc-biotin linker molecules is strongly attached to β -CD SAMs and cannot be removed by rinsing with the buffer. To confirm the multivalency of binding between β -CD SAMs and tetravalent Fc-biotin linker, we did additional experiments, in which rinsing was performed in the presence of competing free β -CDs. Fig. S5 shows typical QCM-D profile obtained during attachment of tetravalent Fc-biotin linker to β -CD SAMs (10 min) followed by the rinsing with the buffer containing 1 mM β -CDs during 20 min until stabilization of the QCM-D signals. We obtained that rinsing with the buffer containing an excess of β -CD leads only to a partial desorption of the linker. In contrast, application of an oxidizing electric field ($E_{ox} = +0.55$ V) after stabilizing F_n and D_n signals leads to the complete detachment of the linker during 2 min. These results suggest that tetravalent Fc-biotin linker interacts with β -CD SAMs through multivalent host-guest (β -CD/Fc) interactions.

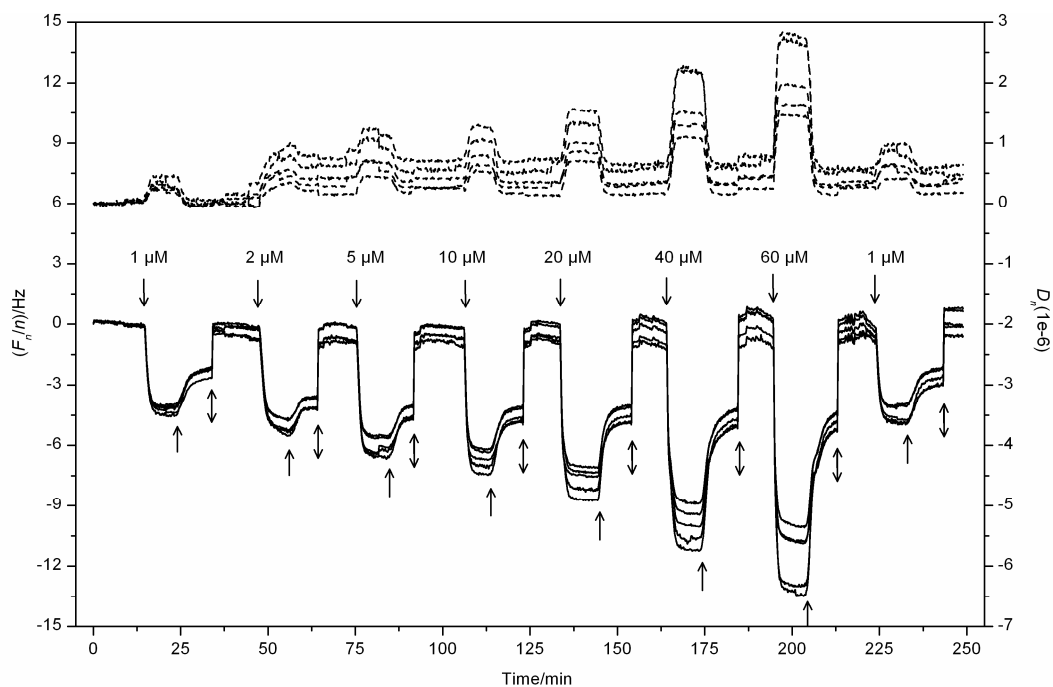


Fig. S2. Frequency F_n/n (solid) and dissipation D_n (dashed) recorded at six overtones $n=3, 5, 7, 9, 11, 13$ (frequency and dissipation shifts increase with overtone number) during reversible attachment of tetravalent Fc-biotin linker injected in different concentrations (1 – 60 μM) at $\beta\text{-CD}$ SAMs; \downarrow – linker injection, \uparrow – buffer rinsing, \updownarrow – 2 min applying +0.55 V; 24 $^\circ\text{C}$, 50 $\mu\text{L}/\text{min}$, 10 mM HEPES with 0.15 M NaCl, pH 7.0 (linker solution contained 1 mM $\beta\text{-CD}$).

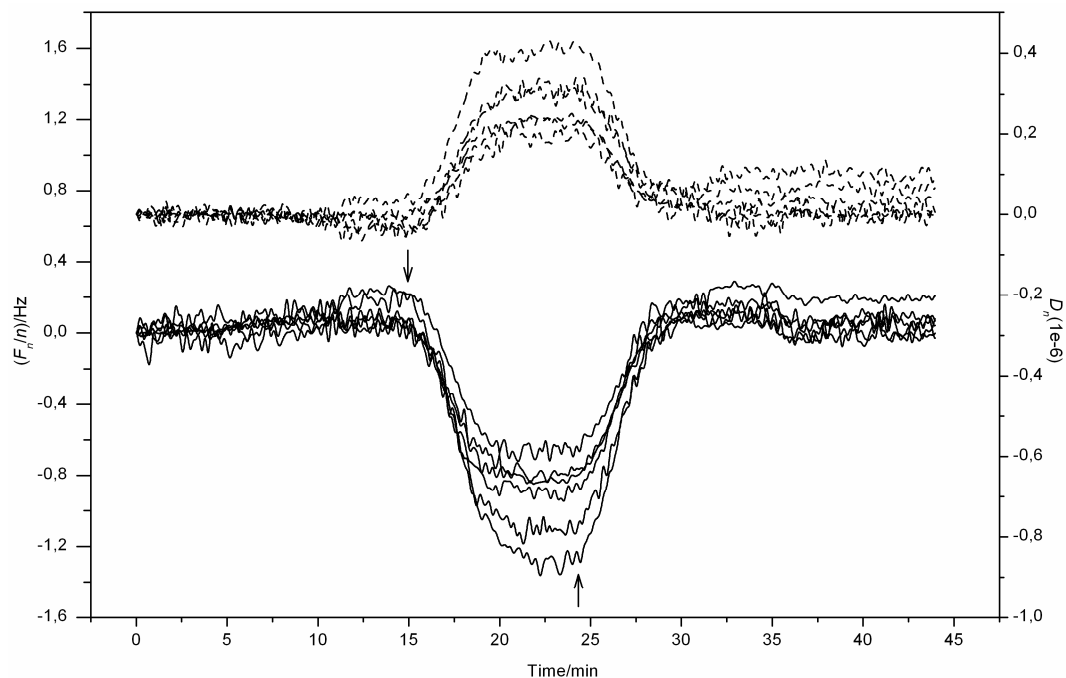


Fig. S3. Frequency F_n/n (solid) and dissipation D_n (dashed) recorded at six overtones $n=3, 5, 7, 9, 11, 13$ (frequency and dissipation shifts increase with overtone number) during attachment of tetravalent Fc-biotin linker to unmodified pegylated SAMs; \downarrow – linker injection, \uparrow – buffer rinsing, 24 $^\circ\text{C}$, 50 $\mu\text{L}/\text{min}$, 10 mM HEPES with 0.15 M NaCl, pH 7.0 (linker solution contained 1 mM $\beta\text{-CD}$).

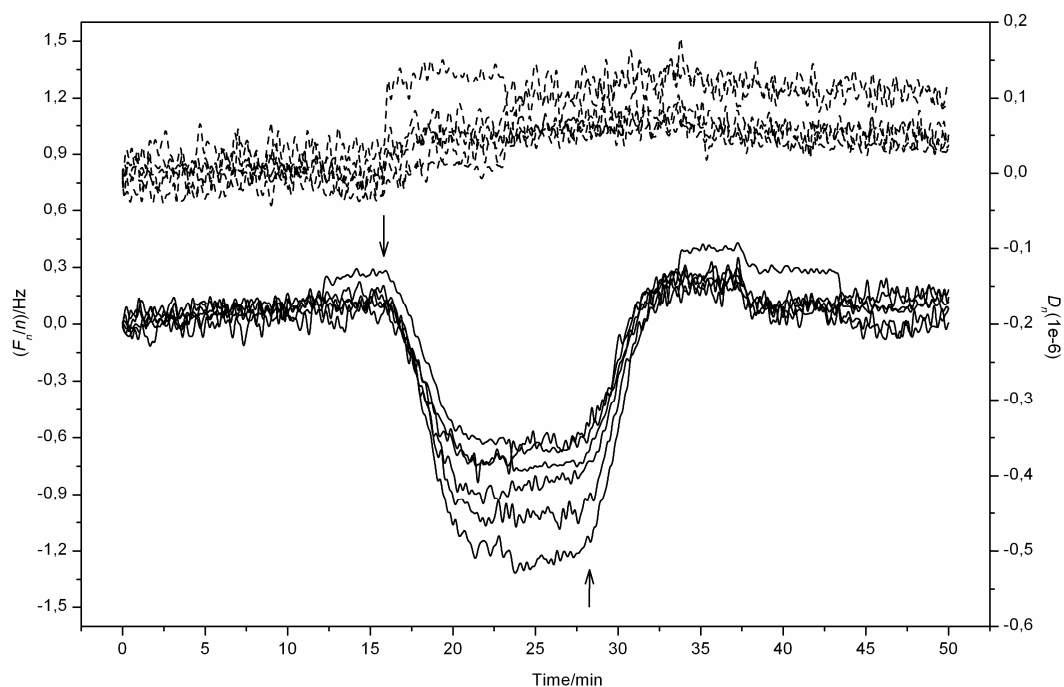


Fig. S4. Frequency F_n/n (solid) and dissipation D_n (dashed) recorded at six overtones $n=3, 5, 7, 9, 11, 13$ (frequency and dissipation shifts increase with overtone number) during attachment of SA to β -CD SAMs; \downarrow – SA injection, \uparrow – buffer rinsing, 24 °C, 50 μ L/min, 10 mM HEPES with 0.15 M NaCl, pH 7.0.

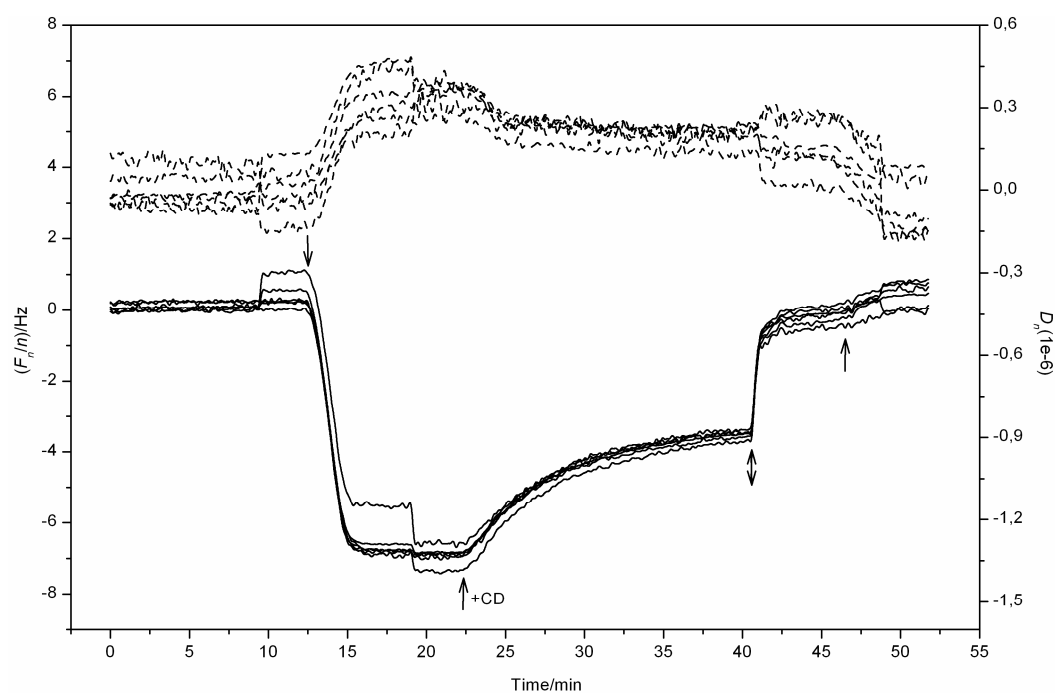


Fig. S5. Frequency F_n/n (solid) and dissipation D_n (dashed) recorded at six overtones $n=3, 5, 7, 9, 11, 13$ (frequency and dissipation shifts increase with overtone number) during attachment of tetravalent Fc-biotin linker to β -CD SAMs followed by rinsing with the buffer containing free β -CDs (1 mM), applying oxidizing electric field ($E_{ox} = +0.55$ V) and rinsing with the buffer without β -CDs; \downarrow – linker injection, \uparrow +CD – rinsing with buffer containing β -CDs, \downarrow – 2 min applying +0.55 V, \uparrow – rinsing with buffer without β -CDs; 24 °C, 50 μ L/min, 10 mM HEPES with 0.15 M NaCl, pH 7.0 (linker solution contained 1 mM β -CD).

6. SPR imaging in ellipsometric mode

Describing the instrument set-up in detail as well as data acquisition and optical modeling is far beyond the scope of this communication and will be the objective of another article in preparation. Briefly, the instrument used was an imaging null-ellipsometer EP3 (Nanofilm, Germany) equipped with an SPR cell, using the Kretschmann setup⁸ where a 60° SF-10 prism is attached to a home-made microfluidic flow cell. The instrument was used in total internal reflection mode and both the intensity and the phase changes of the reflected light were monitored and converted into two ellipsometric angles Ψ and Δ . The data were acquired and evaluated by EP3View V235 Software (Nanofilm, Germany). For modeling, EP4Model 1.0.1 software (Nanofilm, Germany) was used. A xenon lamp was used as a light source, and the wavelength was 630.2 nm as selected by an interference filter. Combining ellipsometry with SPR has been discussed earlier⁹ and a few examples of its use in biomolecular interaction analysis have been reported¹⁰. In the EP3 setup, it is also possible to resolve the surface laterally with about 1 μm resolution, thus enabling to monitor interaction occurring in different regions of the surface simultaneously.

Linker/SA arrays were fabricated using PDMS microchannels to pattern the surface of SPR sensor substrates consisting of a gold film deposited on SF-10 glass. To generate the array, a β -CD SAMs was formed *ex situ* on the gold film following the procedure previously described in Section 2. PDMS microchannels that had been fabricated using a 3-D silicon mask were then placed on the surface and the whole assembly was mounted in the SPR imaging cell using a procedure similar to the one described previously¹¹. The microchannels were composed of a series of 3 parallel 350 μm wide channels, each fitted with inlet and outlet at their ends for sample introduction using a peristaltic pump.

All SPR-ellipsometric experiments were repeated at least three times. The attachment, detachment and mapping steps were performed in 10 mM HEPES buffer containing 0.15 M NaCl (pH 7.0). The concentration of SA in the buffer was 1 mg L⁻¹. The concentration of tetravalent Fc-biotin linker in 10 mM HEPES buffer with 0.15 M NaCl (pH 7.0) containing 1 mM β -CD was 5 μM . Immobilization of the linker and SA was carried out step by step in the channels by flowing the solution through the channels at a flow rate of 50 $\mu\text{L min}^{-1}$. Attachment of both linker and SA was performed during 10 min followed by buffer rinsing (50 $\mu\text{L min}^{-1}$) until stabilization of the optical signals. Simultaneously, it was possible to monitor in situ the Ψ and Δ variations induced by the binding of linker and SA on the β -CD SAMs. This kinetic monitoring was performed at different angles of incidence (AOI) from 56° to 59°. The SPR cell design also allowed to record AOI spectrum, that is the variation of Ψ and Δ for different AOI ranging from 56° to 59° by steps of 0.2°. These experiments were systematically performed for each step of the assembly build-up on region of interest (ROI) that were selected for the relevant parts within the microchannels. Fitting for each step the experimental data with adequate optical models allowed us to determine the optical properties (n and k) of each material as well as the thickness of each layer (Table 1). Using De Feijter relation,¹² it was then possible to extract the optical mass of linker/SA layer:

$$m = d(n - n_{\text{solvent}})/(dn/dc) \quad (4)$$

with m , d , n and dn/dc being respectively adsorbed mass, thickness, refractive index (were taken from Table S1) and refractive index increment. Since linker mass represents only 15-18% of linker/SA mass (according to QCM-D data), we assumed $(dn/dc)_{\text{linker/SA}}$ equal to $(dn/dc)_{\text{SA}}$, which was determined to be 0.180 cm³/g.¹³

Because each channel was independent, different solutions could be introduced and immobilized within each channel. After Linker/SA attachment, the PDMS microchannels were removed from the modified surface. The resulting array was then placed without drying into a home-made flow cell for imaging experiments. Imaging experiments were realized in

the buffer at a flow rate of $50 \mu\text{L min}^{-1}$. AOI spectrums of selected ROI were performed and fitted allowing to check linker/SA film thickness and optical properties. Alternatively, Ψ and Δ maps were recorded at a fixed AOI = 56.8° , from which thickness maps could be extracted by fitting on the basis of the multilayer optical model previously elaborated (Table S1). After mapping, resulting array was mounted without drying in the electrochemical cell described in Section 3 to perform the *ex situ* detachment. After the electrochemical detachment made while stirring during 2×20 min, the sample was mounted again into the home-made flow cell to repeat Ψ and Δ mapping in the buffer under flow conditions ($50 \mu\text{L min}^{-1}$) and extract thickness the map at the same AOI = 56.8° .

Fig. S6 shows the MSE maps obtained in parallel with thickness maps presented in the main text of the manuscript (Fig. 3) using the model described in Table S1. MSE was defined by the EP4Model 1.0.1 software as

$$MSE(d) = \frac{1}{N-L-1} \sum \left(\frac{\Delta_i - \Delta(d)_i}{\delta\Delta_i} \right)^2 + \left(\frac{\Psi_i - \Psi(d)_i}{\delta\Psi_i} \right)^2 \quad (5)$$

where N is the number of data points, L is the number of fit parameters, d is the calculated thickness, Ψ and Δ are the measured ellipsometric parameters. The sum is taken over all measured points (index i), with σ_i being the measurement error or standard deviation of the i^{th} data point, Δ_i and Ψ_i being measured values and $\Delta(d)_i$ and $\Psi(d)_i$ being calculated values.

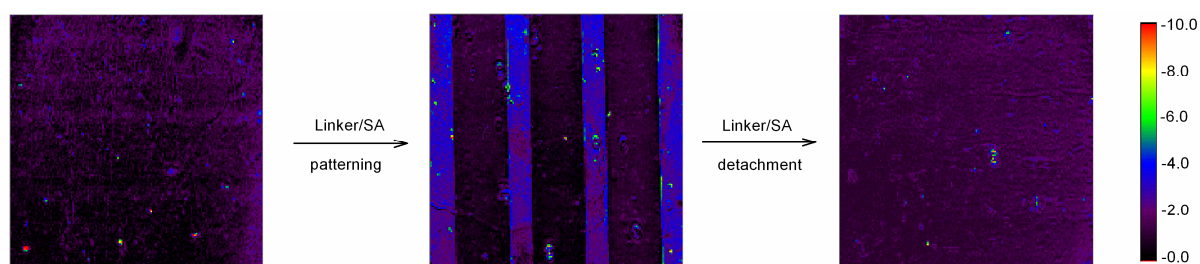


Fig. S6. MSE maps ($1769\mu\text{m} \times 1769\mu\text{m}$) obtained by SPR ellipsometry during mapping layer thicknesses (Manuscript, Fig. 3) after formation of the β -CD SAM on the gold surfaces (left), after linker/SA patterning on the β -CD SAM surface (middle) and after linker/SA electrochemical removal from the β -CD SAM surface (right); 24°C , $50 \mu\text{L/min}$, 10 mM HEPES with 0.15 M NaCl, pH 7.0 (linker solution contained 1 mM β -CD).

Table S1. Procedure used for ellipsometric data modeling.

Modeling sequence	Experiment conditions	Used parameters	Determined parameters	References
1. Bare gold characterization	Bare gold in imaging flow cell, $\lambda=630.2$ nm, $\text{AOI}_{\text{var}}=56-59^\circ$ (step= 0.2°), H_2O	$n_{\text{SF10}}=1.72$ $n_{\text{H2O}}=1.33$	$d_{\text{Au}}=46\pm 1$ nm $n_{\text{Au}}=0.234\pm 0.008$ $k_{\text{Au}}=3.47\pm 0.02$ (determined from 8 experiments)	Gold parameters determined by Nanofilm at $\lambda=633$ nm: $d_{\text{Au}}=45$ nm $n_{\text{Au}}=0.2388$ $k_{\text{Au}}=3.787$
2. β -CD SAMs characterization	β -CD SAM-coated gold in imaging flow cell, $\lambda=630.2$ nm, $\text{AOI}_{\text{var}}=56-59^\circ$ (step= 0.2°), H_2O	$n_{\text{SF10}}=1.72$ $n_{\text{H2O}}=1.33$ $d_{\text{Au}}=46$ nm $n_{\text{Au}}=0.234$ $k_{\text{Au}}=3.47$	$d_{\beta\text{-CD SAM}}=3.7\pm 0.3$ nm $n_{\beta\text{-CD SAM}}=1.50\pm 0.02$ $k_{\beta\text{-CD SAM}}=0.003\pm 0.001$ (determined from 15 experiments)	$d_{\text{HS-C11-OEG4-OH}^-}=2.3$ nm ¹⁴ $d_{\text{HS-C11-OEG6-OH}^-}=2.9$ nm ¹⁴ $d_{\beta\text{-CD}}=0.8$ nm ¹⁵ $n_{\text{alkanethiols}}=1.50$ ¹⁶ $\epsilon_{\beta\text{-CD}}=2.3$ ¹⁵
3. Buffer characterization	β -CD SAM-coated gold in imaging flow cell, $\lambda=630.2$ nm, $\text{AOI}_{\text{var}}=56-59^\circ$ (step= 0.2°), buffer	$n_{\text{SF10}}=1.72$ $d_{\text{Au}}=46$ nm $n_{\text{Au}}=0.234$ $k_{\text{Au}}=3.47$ $d_{\beta\text{-CD SAM}}=3.7$ nm $n_{\beta\text{-CD SAM}}=1.50$ $k_{\beta\text{-CD SAM}}=0.003$	$n_{\text{buffer}}=1.3335\pm 0.0003$ (determined from 11 experiments)	
4. Linker/SA characterization	β -CD SAM-coated gold with linker/SA pattern in imaging flow cell, $\lambda=630.2$ nm, $\text{AOI}_{\text{var}}=56-59^\circ$ (step= 0.2°), buffer	$n_{\text{SF10}}=1.72$ $n_{\text{buffer}}=1.3335$ $d_{\text{Au}}=46$ nm $n_{\text{Au}}=0.234$ $k_{\text{Au}}=3.47$ $d_{\beta\text{-CD SAM}}=3.7$ nm $n_{\beta\text{-CD SAM}}=1.50$ $k_{\beta\text{-CD SAM}}=0.003$	$d_{\text{linker/SA}}=3.0\pm 0.3$ nm $n_{\text{linker/SA}}=1.48\pm 0.02$ $k_{\text{linker/SA}}=0.005\pm 0.2$ (determined from 5 experiments)	$n_{\text{SA}}=1.45$ ¹⁶ $d_{\text{linker/SA}}=2.7$ nm ^{17*}
5. Building thickness maps	- β -CD SAM-coated gold; - β -CD SAM-coated gold with linker/SA pattern; - β -CD SAM-coated gold after the detachment of linker/SA pattern in imaging flow cell, $\lambda=630.2$ nm, $\text{AOI}=56.8^\circ$, buffer	$n_{\text{SF10}}=1.72$ $n_{\text{buffer}}=1.3335$ $d_{\text{Au}}=46$ nm $n_{\text{Au}}=0.234$ $k_{\text{Au}}=3.47$ $n_{\text{organic layer}}=1.49$ ** $k_{\text{organic layer}}=0.004$ **	$d_{\text{organic layer}} \rightarrow$ thickness maps***	

* The linker in this work is 1-biotin-3-(3,5-di(tetraethylene glycol adamantly ether)) benzyl amide.

** $n_{\text{organic layer}}$ and $k_{\text{organic layer}}$ were taken as average values between n and k obtained for β -CD SAM layer and for linker/SA layer.

***To obtain thickness maps, a single procedure was used for all samples (β -CD SAM-coated gold, β -CD SAM-coated gold with linker/SA pattern, β -CD SAM-coated gold after the detachment of linker/SA pattern), modeled by gold substrate and one organic layer. Therefore, the pattern lines (Manuscript, Fig. 3) represent thicknesses of the organic layer, which is β -CD SAM + linker/SA.

7. Characterization of linker/SA complex

QCM-D characterization. In order to understand whether the amount of surface-attached SA is controlled by the amount of linker or by the steric hindrance in our system, we studied the correlation between the amount of linker attached to β -CD SAMs and the amount of SA attached to linker-covered β -CD SAMs using QCM-D (Fig. S7). One way to perform this experiment is to vary the time of linker adsorption. Because of the rather fast kinetics of linker adsorption (~ 3 min is needed to achieve a plateau), we chose another way based on varying the number of β -CD groups in β -CD SAMs. With the method used in this work to prepare β -CD SAMs, which is briefly described in Section 2, it is possible to obtain SAMs containing the desired amounts of azide groups by choosing an appropriate thiol-PEG-N₃/thiol-PEG ratio during SAMs formation.² Moreover, the more azide groups are present in SAMs, the more β -CD groups can be clicked to these SAMs, with saturation being at thiol-PEG-N₃ surface fraction of 15% (Fig. S7a).² We found that the amount of linkers attached to β -CD SAMs (Fig. S7b) reaches a plateau at the same thiol-PEG-N₃ surface fraction ($\sim 15\%$) as compared to the amount of β -CD groups (Fig. S7a). In contrast, the amount of surface-attached SA (Fig. S7c) becomes constant at much lower thiol-PEG-N₃ surface fraction ($\sim 5\%$). The comparison of Fig. S7b and Fig. S7c shows that the amount of surface-attached SA is controlled by the amount of surface-attached linker when the amount of the linker is less than its half-maximum (~ 35 ng/cm²). In contrast, the amount of surface-attached SA is controlled by the steric hindrance in the SA monolayer when the amount of the linker is higher than its half-maximum.

All QCM-D and ellipsometric experiments presented in this work were performed using samples prepared at thiol-PEG-N₃ surface fraction of $\sim 15\%$ (the dashed area in Fig. S7), with thiol-PEG-N₃/thiol-PEG ratio in solution being of 20% (see Section 2). For these samples, the amount of SA attached to the surface is limited by the steric hindrance in the protein monolayer and not (any more) by the amount of linker. Taking into account the absence of non-specific adsorption of SA (Fig. S4) and that the same amount of SA can be attached to the surface covered with two-times less amount of the linker (Fig. S7), we can conclude that the ratio of linker molecules to SA molecules is >1 in our system.

SPR ellipsometry characterization. In order to confirm the steric hindrance in SA monolayer evidenced by QCM-D (Fig. S7), we determined the optical (dry) mass of surface-attached SA by SPR ellipsometry. Using two different AOI spectrums, first obtained after linker adsorption and second obtained after SA attachment, and model consisting of gold substrate, β -CD SAM layer, linker layer and SA layer, we determined separately thicknesses of linker and SA layers (using the same procedure as described in Section 6). Using previously determined parameters of gold substrate (Table S1, row N°1) and β -CD SAM layer (Table S1, row N°2), we found from several ellipsometric experiments $d_{linker} = 0.5 \pm 0.2$ nm and $d_{SA} = 2.6 \pm 0.3$ nm. Using the de Feijter relation (4) (dn/dc of SA is 0.180 cm³/g¹³), we obtained the optical (dry) mass of SA equal to 210 ± 20 ng/cm². This value corresponds to a densely packed SA monolayer^{6,13,18} thus confirming the steric hindrance in SA monolayer demonstrated by QCM-D monitoring.

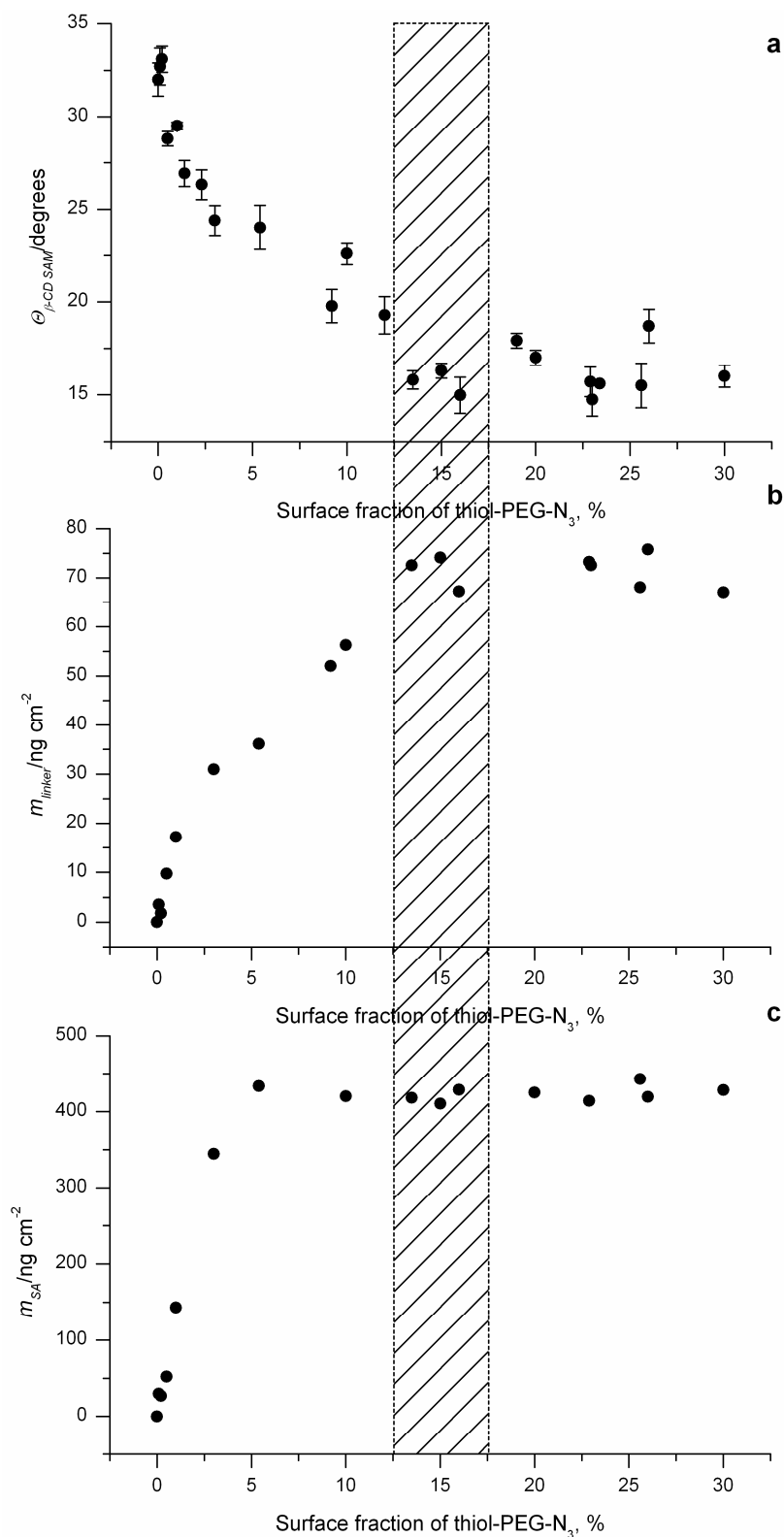


Fig. S7. Influence of thiol-PEG-N₃ surface fraction (determined by contact angle measurements²) on the amount of β -CD clicked to SAMs (characterized by contact angle measurements², new points are added to the plot previously reported²) (a), on the amount of the attached linker (acoustic masses determined by QCM-D) (b) and on the amount of SA attached to the linker-covered β -CD SAMs (acoustic masses determined by QCM-D) (c); dashed area indicates the range of samples used in this work; QCM-D conditions: 24 °C, 50 μ L/min, 10 mM HEPES with 0.15 M NaCl, pH 7.0 (linker solution contained 1 mM β -CD).

References

1. M. Galibert, P. Dumy, D. Boturyn, *Angew. Chem.*, 2009, **121**, 2614; *Angew. Chem. Int. Ed.*, 2009, **48**, 2576.
2. G. V. Dubacheva, A. Van Der Heyden, P. Dumy, O. Kaftan, R. Auzély-Velty, L. Coche-Guerente and P. Labbe, *Langmuir*, 2010, **26**, 13976.
3. J. Hodak, R. Etchenique, E. J. Calvo, *Langmuir*, 1997, **13**, 2708.
4. Ch. A. Nijhuis, F. Yu, W. Knoll, J. Huskens and D. N. Reinhoudt, *Langmuir*, 2005, **21**, 7866.
5. G. Sauerbrey, *Zeitschrift für Physik A*, 1959, **155**, 206.
6. P. Bingen, G. Wang, N. F. Steinmetz, M. Rodahl, R. P. Richter, *Analytical Chemistry*, 2008, **80**, 8880.
7. M. Rodahl, B. Kasemo, *Sensors and Actuators A: Physical*, 1996, **54**, 448.
8. H. Raether, *Surface plasmons on smooth and rough surfaces and on gratings*. Springer, Berlin, 1988.
9. F. Abelès, *Surf. Sci.*, 1976, **56**, 237.
10. M. Poksinski and H. Arwin, *Thin Solid Films*, 2004, **455-456**, 361; P. Westphal and A. Bornmann, *Sens. Actuators B*, 2002, **84**, 278; G. Klenkar, B. Liedberg, *Anal. Bioanal. Chem.*, 2008, **391**, 1679.
11. E. A. Smith, W. D. Thomas, L. L. Kiessling and R. M. Corn, *J. Am. Chem. Soc.*, 2003, **125**, 6140.
12. J. A. Feijter, J. Benjamins, F. A. Veer, *Biopolymers*, 1978, **17**, 1759.
13. E. Reimhult, C. Larsson, B. Kasemo, F. Höök, *Anal. Chem.*, 2004, **76**, 7211.
14. C. Pale-Crosdemange, E. S. Simon, K. L. Prime and G. M. Whitesides, *J. Am. Chem. Soc.*, 1991, **113**, 12.
15. M. Frasconi and F. Mazzei, *Nanotechnology*, 2009, **20**, 285502.
16. J. Spinke, M. Liley, F. Schmitt, H. Guder, L. Angermaier and W. Knoll, *J. Chem. Phys.*, 1993, **99**, 7012.
17. M. J. W. Ludden, M. Péter, D. N. Reinhoudt and J. Huskens, *Small*, 2006, **2**, 1192.
18. Ch. Larsson, M. Rodahl and F. Höök, *Anal. Chem.*, 2003, **75**, 5080.